

Local and global changes to the thermosphere from the dissipation of gravity waves from deep convection

Sharon Vadas

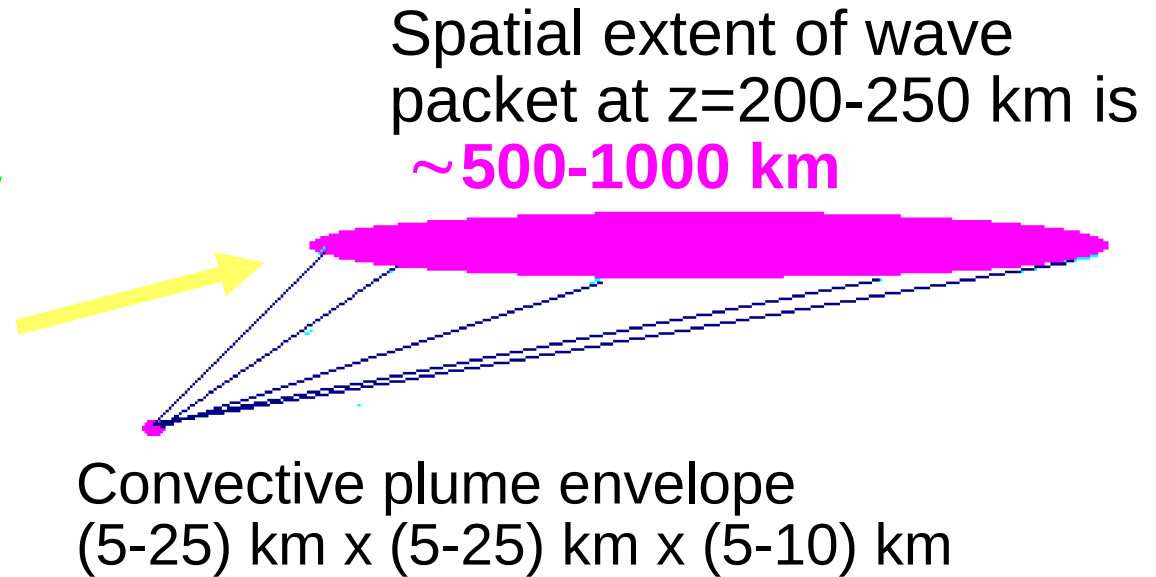
NorthWest Research Associates/CoRA

Gravity Wave Symposium

17 May 2016, Penn State University

GOAL: To model the effect of GWs from deep convection on the thermosphere globally

Due to wave dispersion, a GW packet spreads out to a large volume in thermosphere



Not currently possible to simulate both the excitation of (resolved) GWs from deep convection and the propagation/dissipation of GWs in thermosphere with a single numerical model

Solution to model the effect on the thermosphere from GWs from deep convection globally as-realistic-as-possible (not using a convective parameterization)

- 1) Obtain IR satellite images that cover the Earth. Pick out convective plumes overshooting the tropopause. Determine updraft velocities from CAPE.
- 2) Use the Vadas (2013) compressible convective plume envelope model to estimate the excited primary GW spectrum for each convective object.
- 3) Build a high-resolution 2800 x 2800 km (40 x 40 x 4km x 6min) box around each convective object. **Ray trace** GWs into thermosphere where they dissipate and/or saturate (Vadas and Fritts, 2005; Vadas and Liu, 2009,2013). Reconstruct the GW field, and calculate the thermospheric body forces and heat/coolings.
- 4) Run TIME-GCM with/without GW forces and with/without the heat/coolings to calculate the local and global effects on the thermosphere

Vadas (2013) compressible **convective plume envelope** model to estimate the excited GWs

In a moist convective system, latent heat/cooling and nonlinear forcing excite GWs (Lane et al, 2001).

Linear dry air GW excitation models implement:

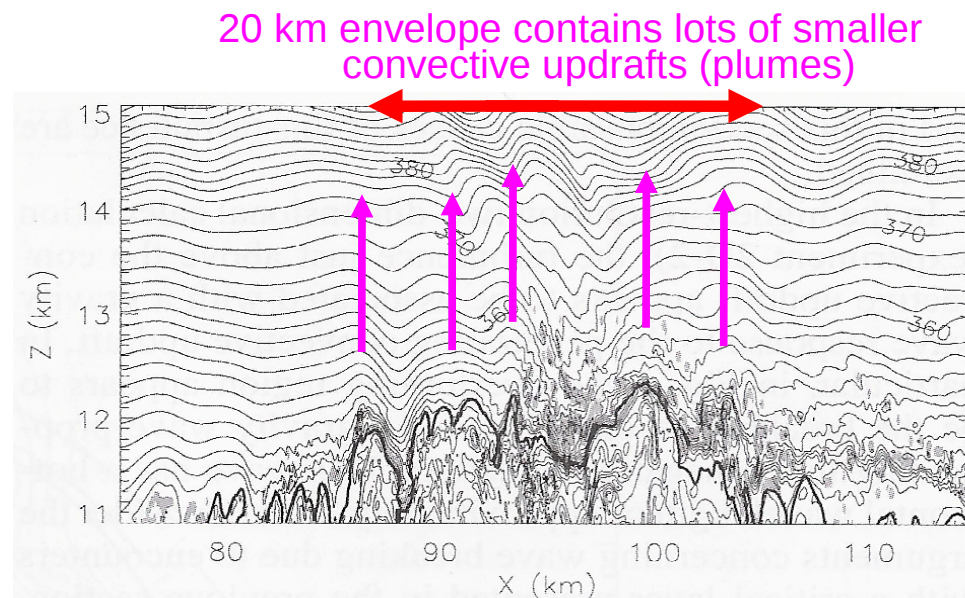
1) **diabatic forcing** (e.g., Alexander et al, 1995; Piani et al, 2000; Walterscheid et al, 2001; Beres, 2004).

2) **convective overshoot** (e.g., Stull, 1976; Vadas and Fritts, 2009; Vadas et al, 2009, 2012, 2014)

Our linear dry air model neglects the small-scale up/downdrafts because the GWs excited by these smaller-scale motions are smaller-scale and cannot propagate into the mesosphere/thermosphere without breaking/dissipating. Includes factor of 1/2 and only “good” for GWs with phase speeds $>20\text{-}25$ m/s (Song et al, 2003; Choi et al, 2007)

Full non-linear 2D
convection model

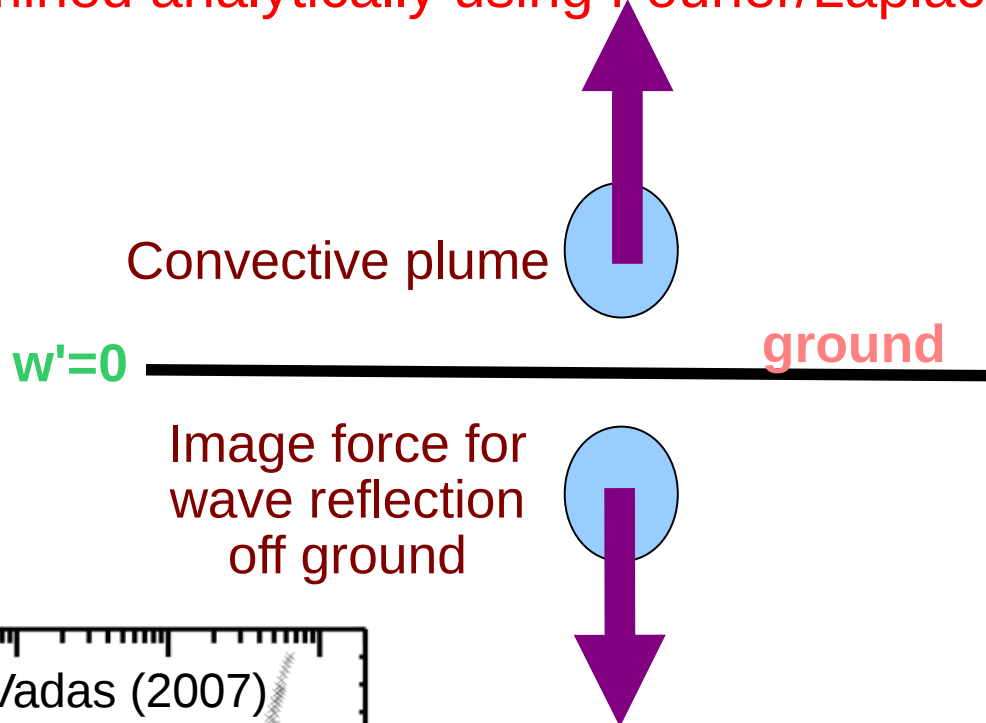
(Lane et al, JAS, 2003)



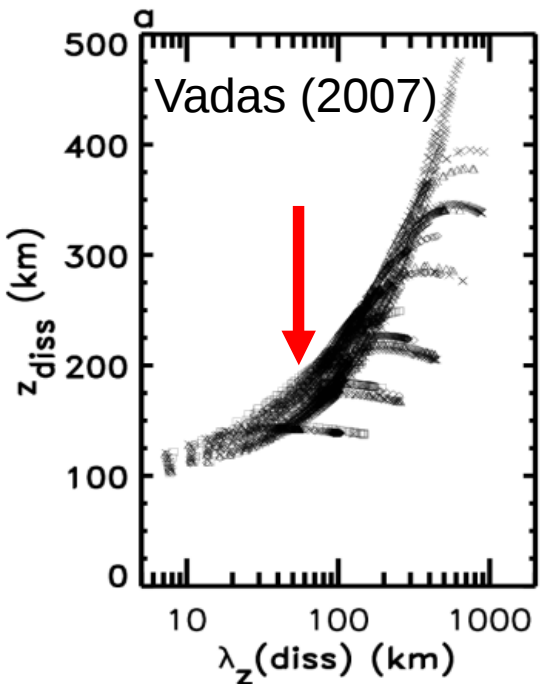
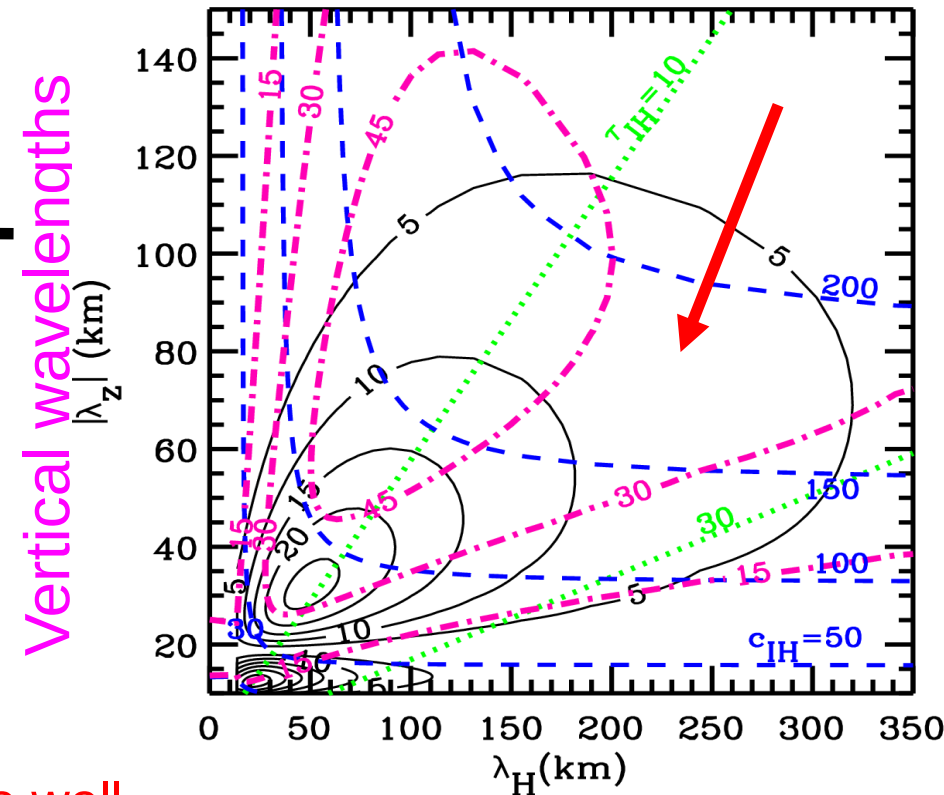
10 July, 1997,
North Dakota
Potential
temperature

Compressible convective plume model:

Convective overshoot is modeled as a vertical body force which neglects small-scale structure and varies as $\cos^2(t/\sigma)$ in time [σ =duration]. Solutions are determined analytically using Fourier/Laplace methods (Vadas, 2013)



Spectrum of GWs excited from a convective plume with a 15 km envelope



GWs which propagate well into the thermosphere are in the tail of the excited GW spectrum ($c_{IH} > 60$ m/s, $\lambda_z > 10$ km)

Horizontal wavenumbers

Vadas and Fritts (2009)

Ray tracing utilizes a dissipative anelastic dispersion relation which includes the effects of kinematic viscosity and thermal diffusivity (Vadas and Fritts, 2005):

$$m^2 = \frac{k_H^2 N^2}{\omega_{Ir}^2 (1 + \delta_+ + \delta^2 / \text{Pr})} \left[1 + \frac{\nu^2}{4\omega_{Ir}^2} \left(\mathbf{k}^2 - \frac{1}{4H^2} \right)^2 \frac{(1 - \text{Pr}^{-1})^2}{(1 + \delta_+/2)^2} \right]^{-1} - k_H^2 - \frac{1}{4H^2}$$

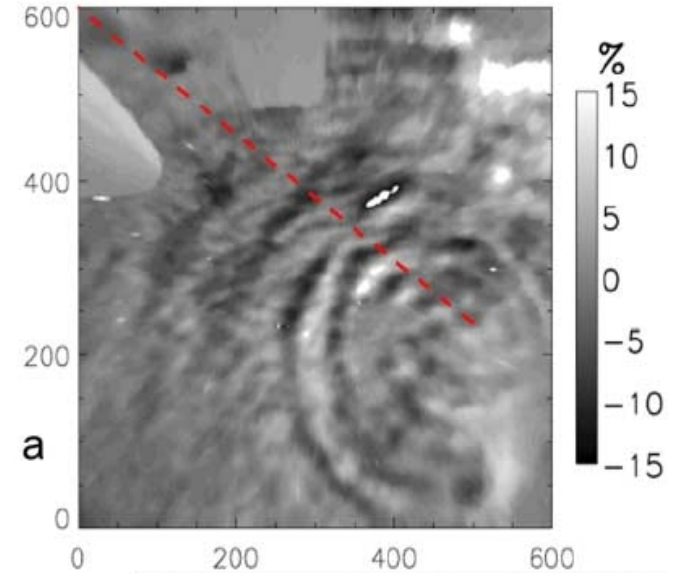
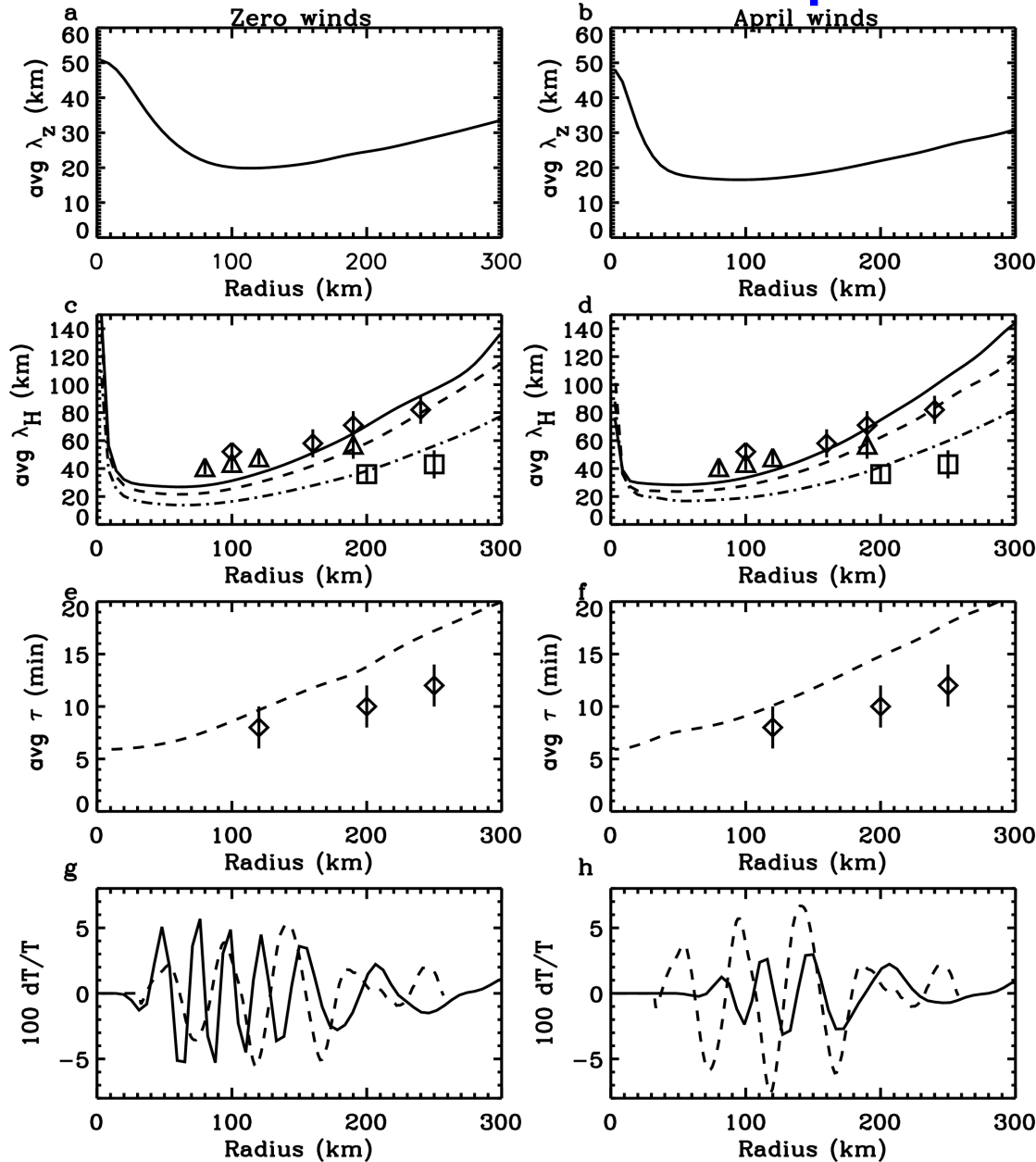
$$\begin{aligned} \mathbf{k} &= (k, l, m), & k_H^2 &= k^2 + l^2, & \omega_{Ir} &= \omega - kU - lV \\ \delta &= \nu m / H\omega_{Ir}, & \delta_+ &= \delta(1 + 1/\text{Pr}), & \nu_+ &= \nu(1 + 1/\text{Pr}) \end{aligned}$$

GW dissipative
dispersion relation

$$\omega_{Ii} = -\frac{\nu}{2} \left(\mathbf{k}^2 - \frac{1}{4H^2} \right) \frac{[1 + (1 + 2\delta) / \text{Pr}]}{(1 + \delta_+/2)}$$

Amplitude decay in time

Comparison between OH airglow data and this convective plume/ray trace model:



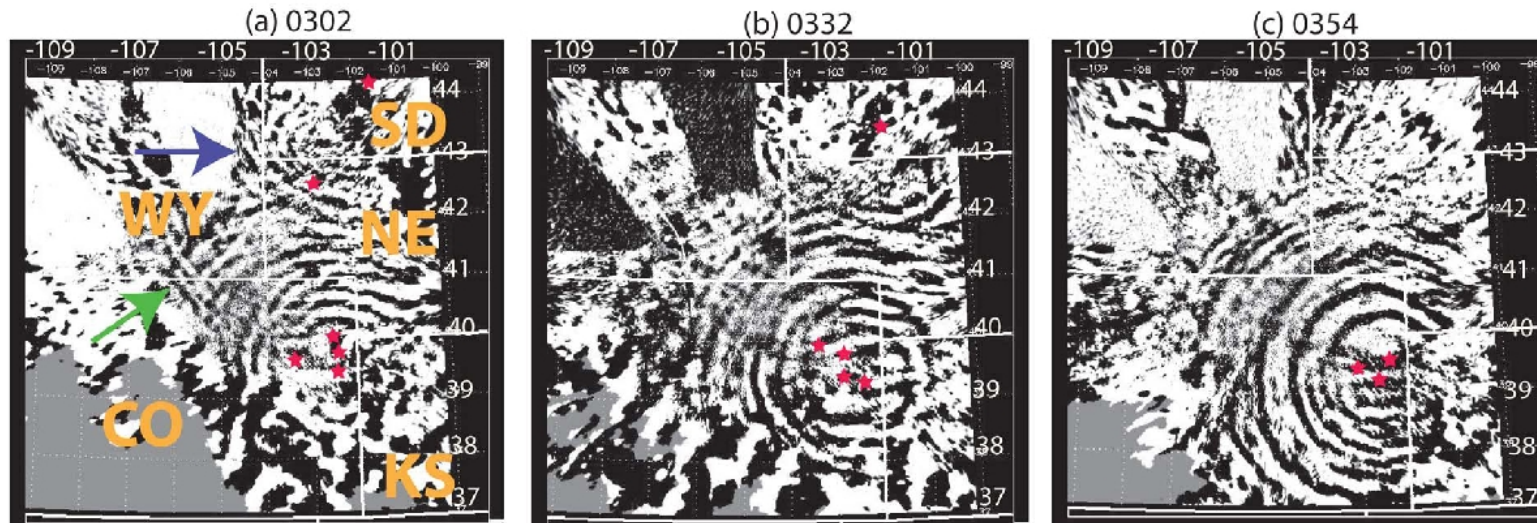
Modeled GWs excited from the convective plume reproduce the data very well, thereby ensuring the scales and amplitudes of the convective plume envelope model are reasonable

11 May 2004 at Yucca Ridge, CO

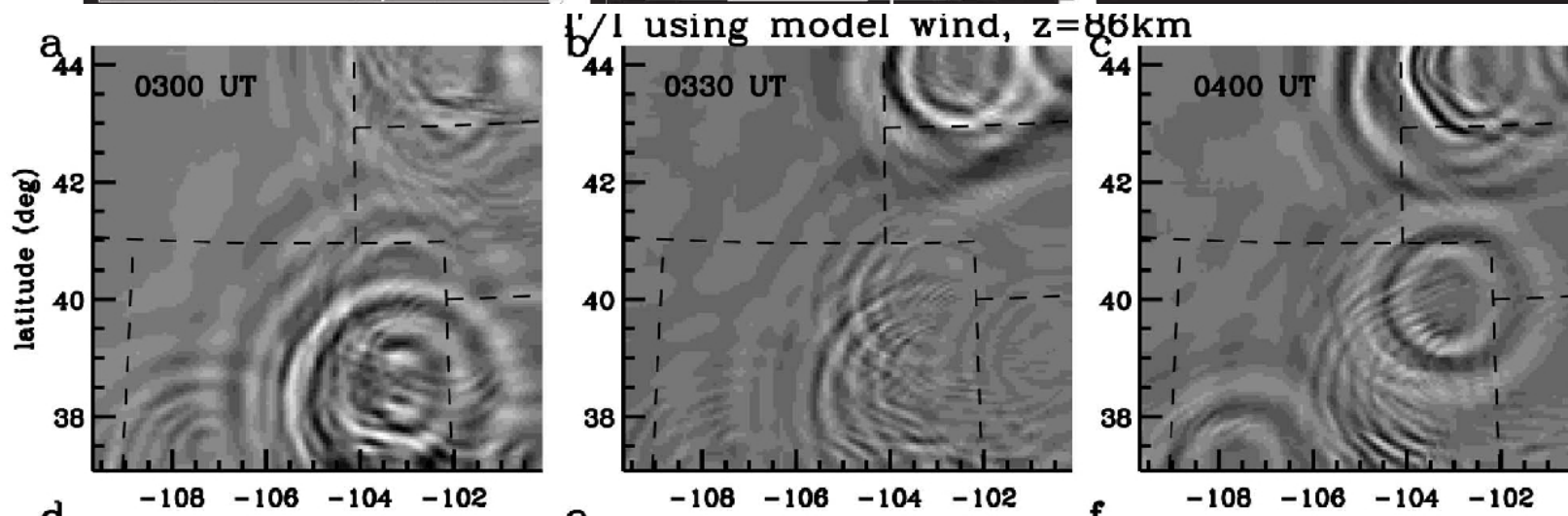
(Vadas, Yue, et al, 2009, JGR)

Comparison between OH airglow data and ray trace convective model data

September 8, Yucca Ridge



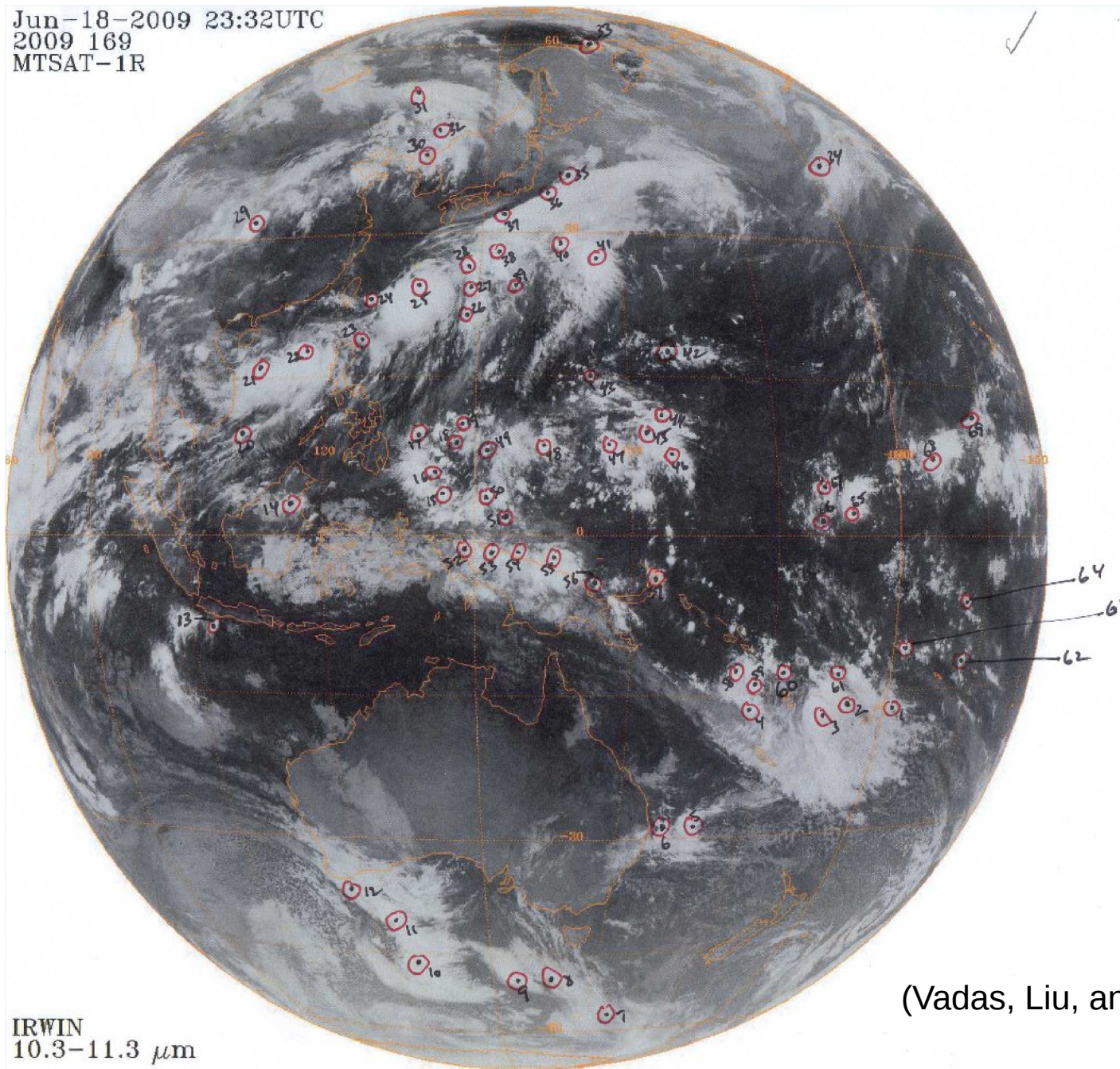
OH data



Convective plume model, ray tracing and reconstruction of GW field

13 days of deep convection globally during 15-27 June 2009

Jun-18-2009 23:32UTC
2009 169
MTSAT-1R



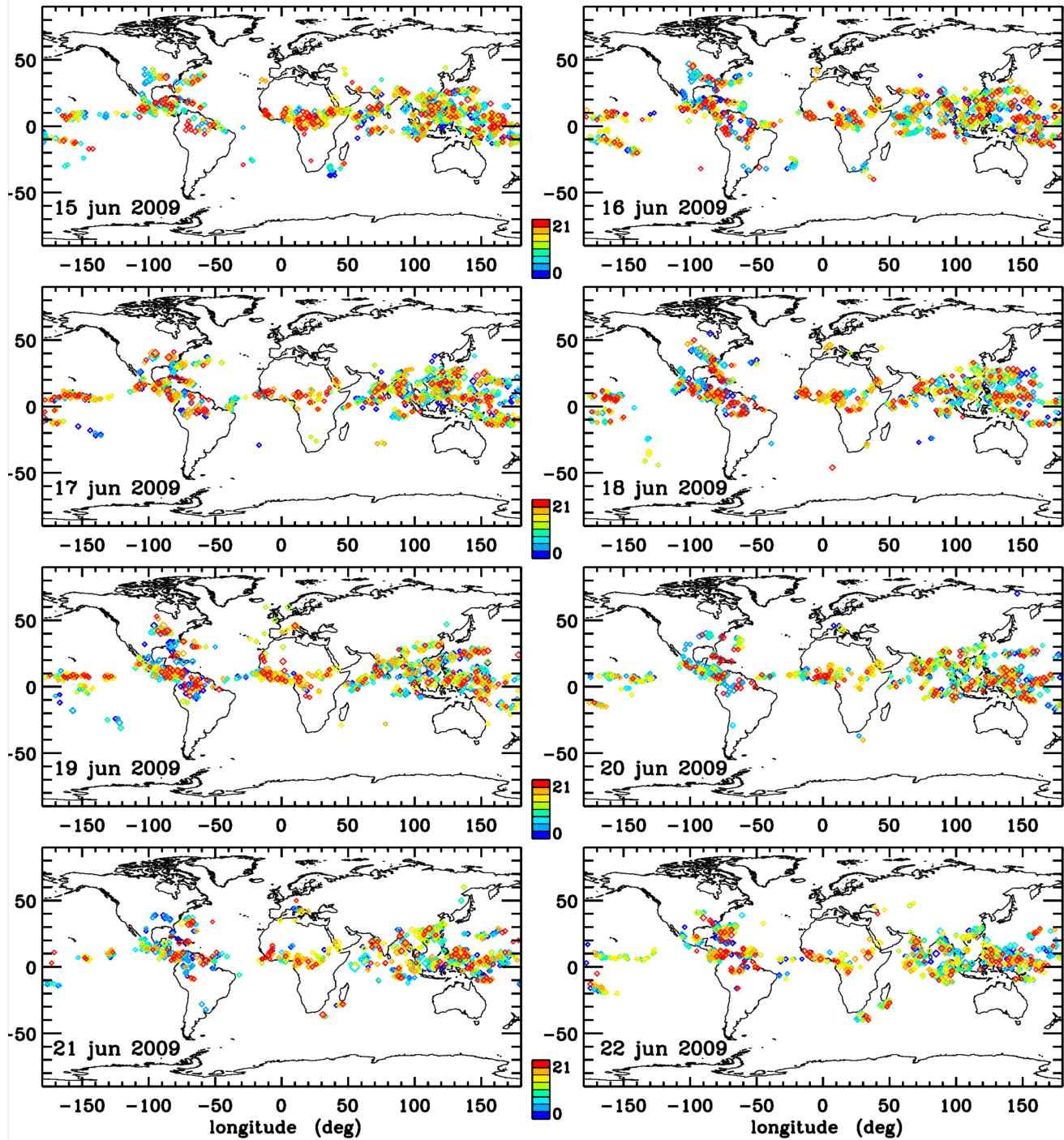
Satellites: GOES-11,
GOES-12, M7, M9, and
MTS

Example:
GMTSAT infrared
satellite image at
23:32 UT on 18
June 2009 showing
the
Indonesian/Australi
an sector

(Vadas, Liu, and Lieberman, 2014, JGR)

IRWIN
10.3-11.3 μm

Convective activity world-wide in June 2009



(Vadas, Liu, and Lieberman, 2014, JGR)

Total body forces and heat/coolings caused by the dissipation and/or saturation of these GWs in the thermosphere:

$$F_{x,\text{tot}} = -\frac{1}{\bar{\rho}} \frac{\partial (\overline{\rho u' w'})}{\partial z}, \quad F_{y,\text{tot}} = -\frac{1}{\bar{\rho}} \frac{\partial (\overline{\rho v' w'})}{\partial z}, \quad (73)$$

Zonal and meridional body forces created from GW dissipation

$$J_{\text{tot}} = -\frac{1}{\rho} \frac{\partial}{\partial z} \left(\frac{\rho T}{\theta} F_{\theta} \right) - \frac{g}{C_p} \frac{F_{\theta}}{\theta} + \frac{\nu}{C_p} \overline{\left(\frac{\partial}{\partial z} \mathbf{v}' \right)^2}, \quad (74)$$

(Becker, 2004)

Heat flux convergence

Buoyancy production of GW kinetic energy

Dissipation of GW kinetic energy due to molecular viscosity

Induced neutral wind and temperature perturbations at z=250 km

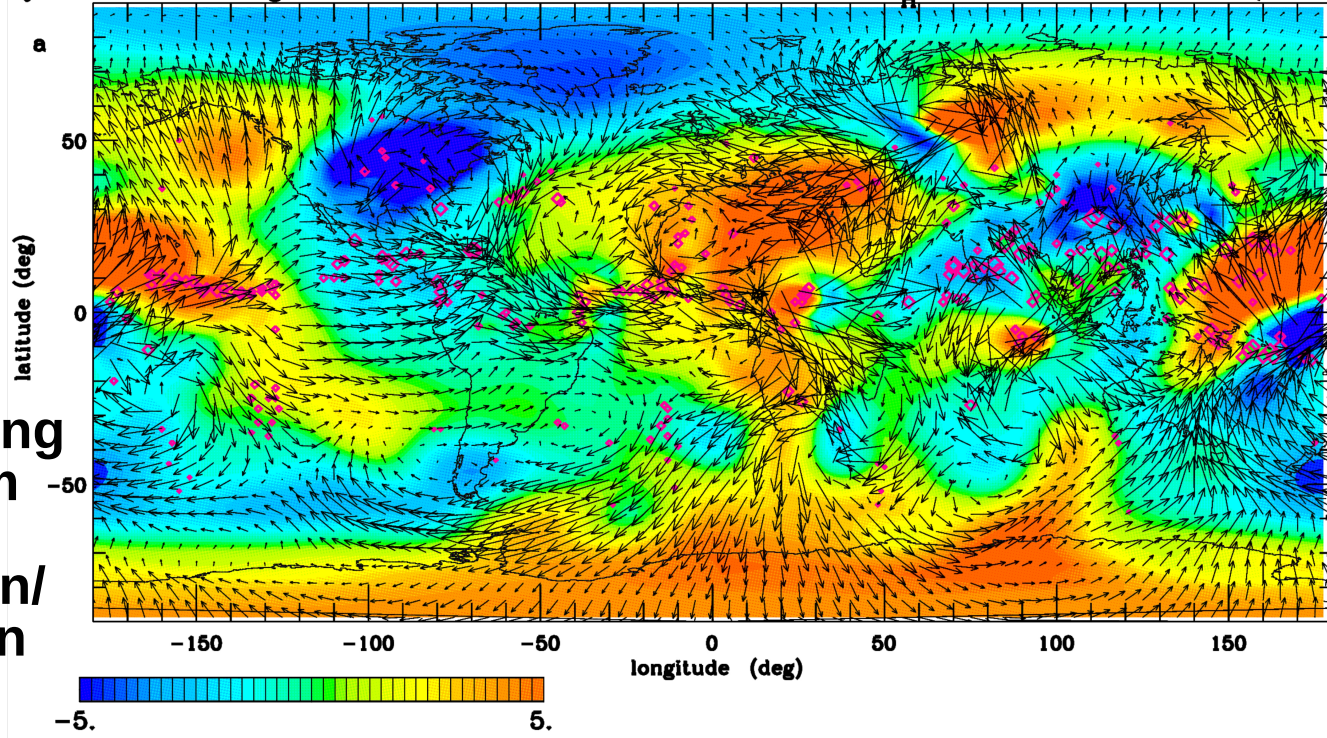
Forces are maximum at z~180-200 km.

u_H' is maximum at z~150-250 km (counter-rotating cells created for each force)

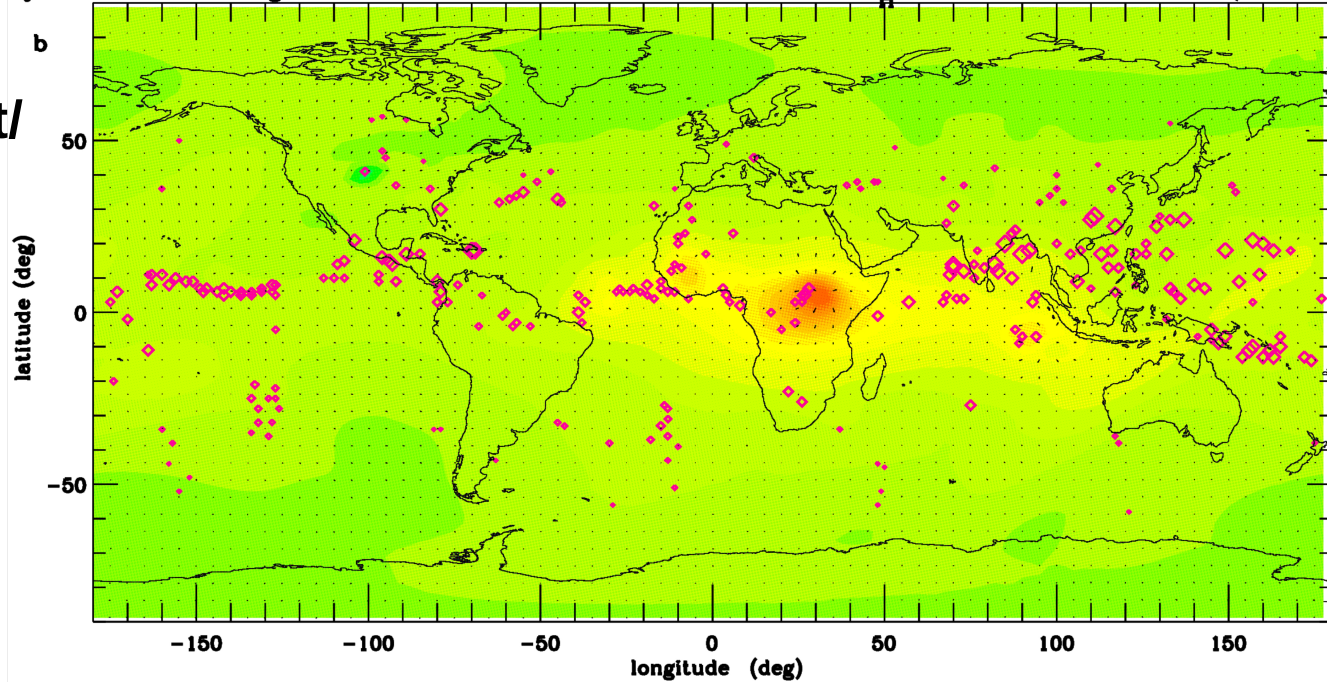
F_x, F_y forcing only from GW dissipation/saturation

GW heat/cooling only (much smaller effect)

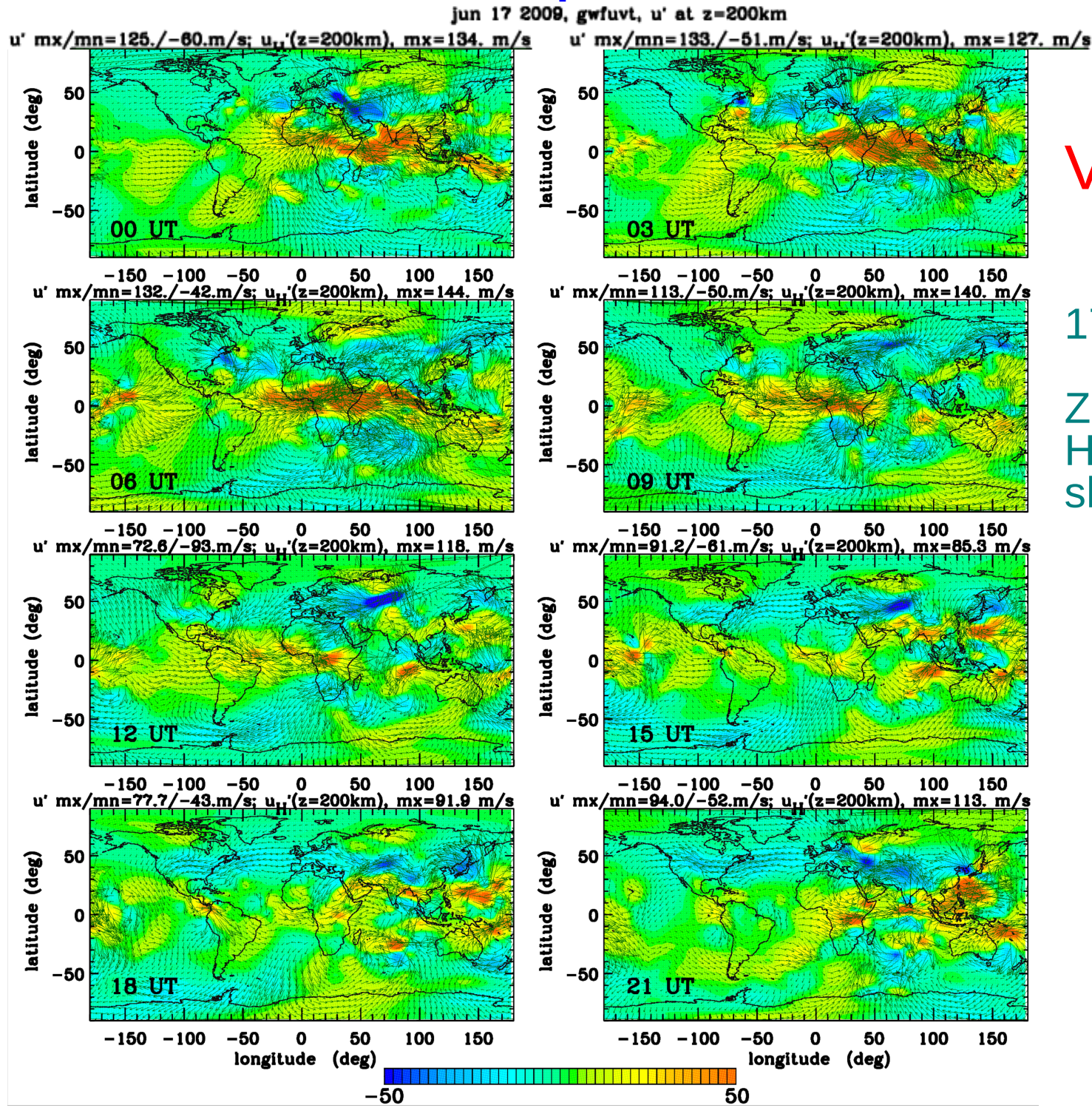
jun 17 2009, 12 UT, gwfv. T' at z=250km, max=15.2 K, min=-8.4 K; u_H' at z=250km, max=76.2 m/s



jun 17 2009, 12 UT, gwft. T' at z=250km, max=5.50 K, min=0.10 K; u_H' at z=250km, max=2.20 m/s



Induced neutral wind perturbations at z=200 km every 3 hours



Variation in time

17 June at z=200 km.

Zonal wind blue to red
Horizontal wind are shown as vectors

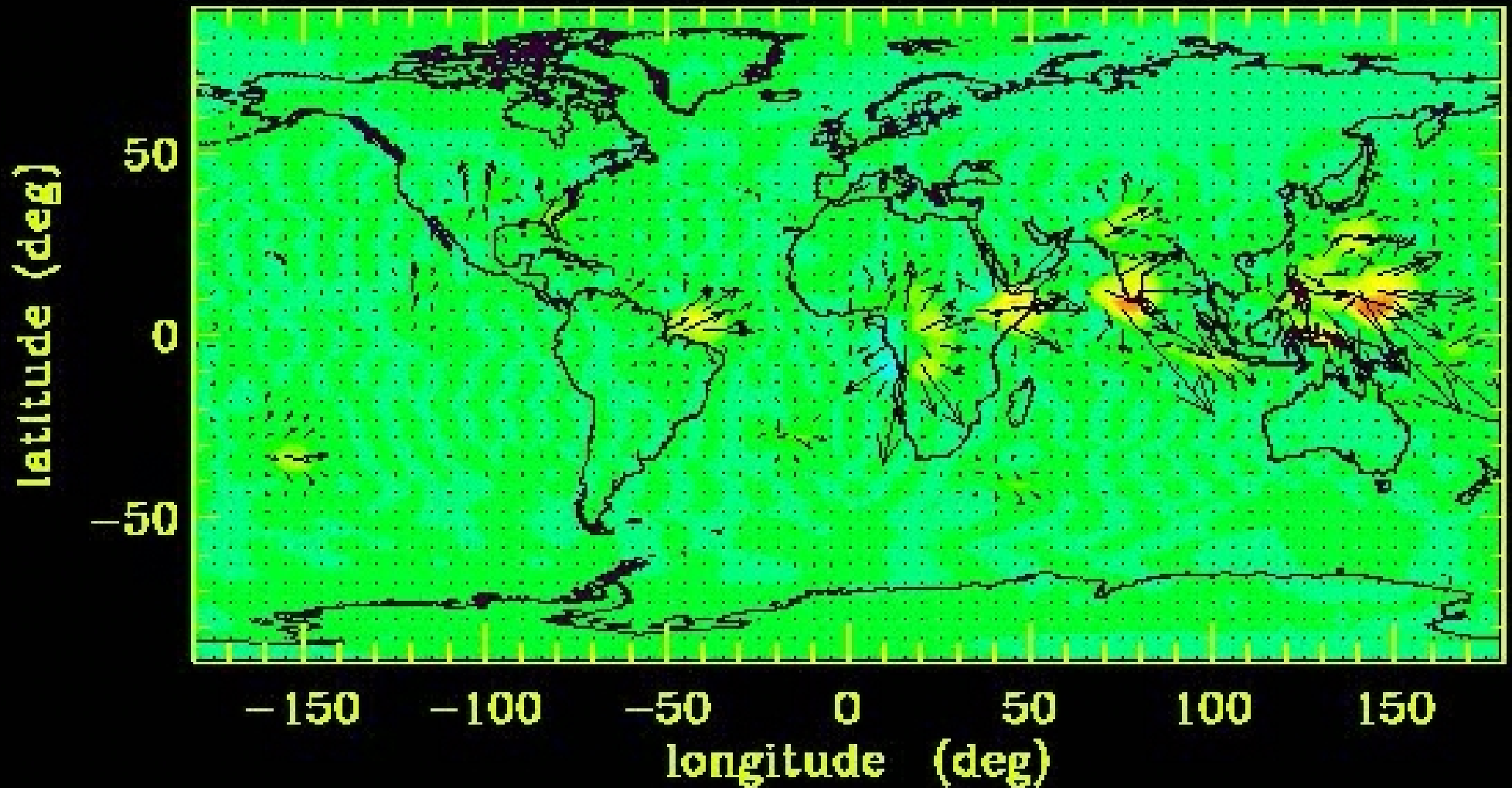
Horizontal wind perturbations vary strongly in time over 3-6 hrs

(Vadas, Liu, and Lieberman, 2014, JGR)

u_{\perp}' movie every hour at $z=200$ km

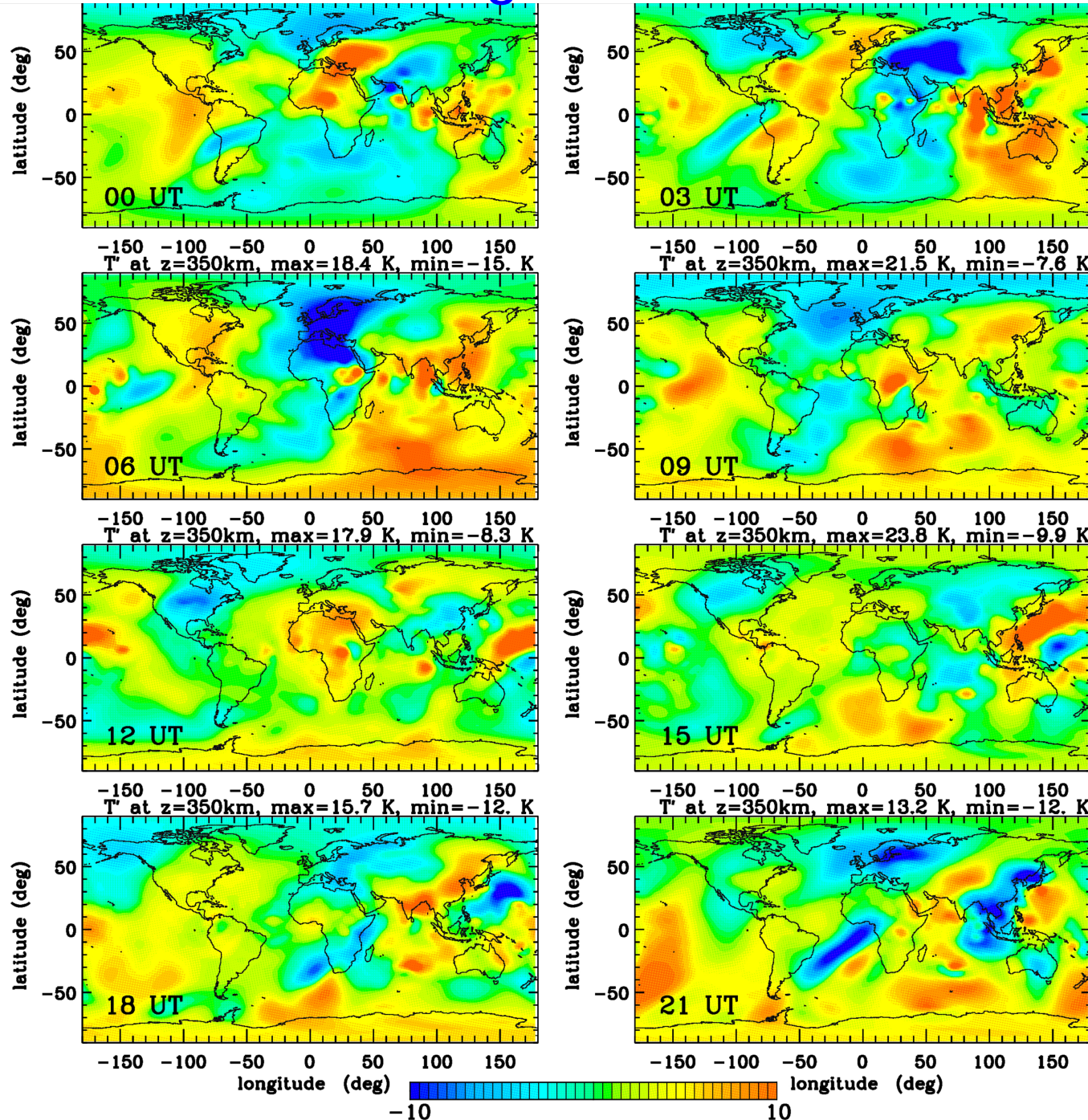
u' mx/mn=50.7/-16.m/s; $u_H'(z=200\text{km})$, mx=64.3 m/s

15 jun 2009 at 00 UT



(Vadas, Liu, and Lieberman,
JGR, 2014)

Wind filtering in the mesopause and lower thermosphere causes the in-situ generation of tides in the thermosphere:

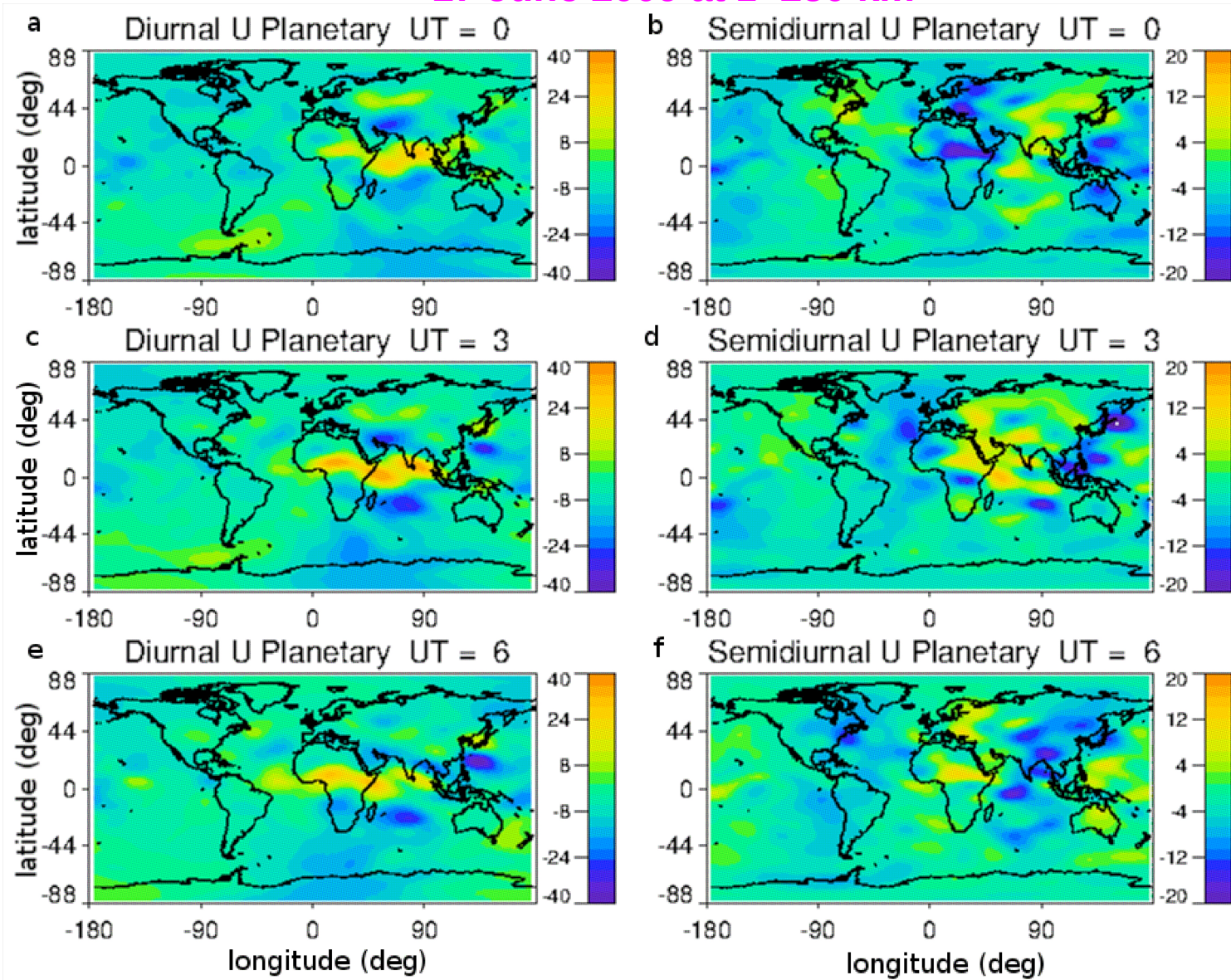


T' at $z=350$ km

(Vadas, Liu, and Lieberman, 2014, JGR)

In-situ generation of planetary scale diurnal and semidiurnal tides in the thermosphere:

17 June 2009 at z=250 km



Planetary-scale eastward and westward diurnal and semidiurnal tides are generated in-situ in thermosphere, with $u' \sim 10-40$ m/s.

Conclusions

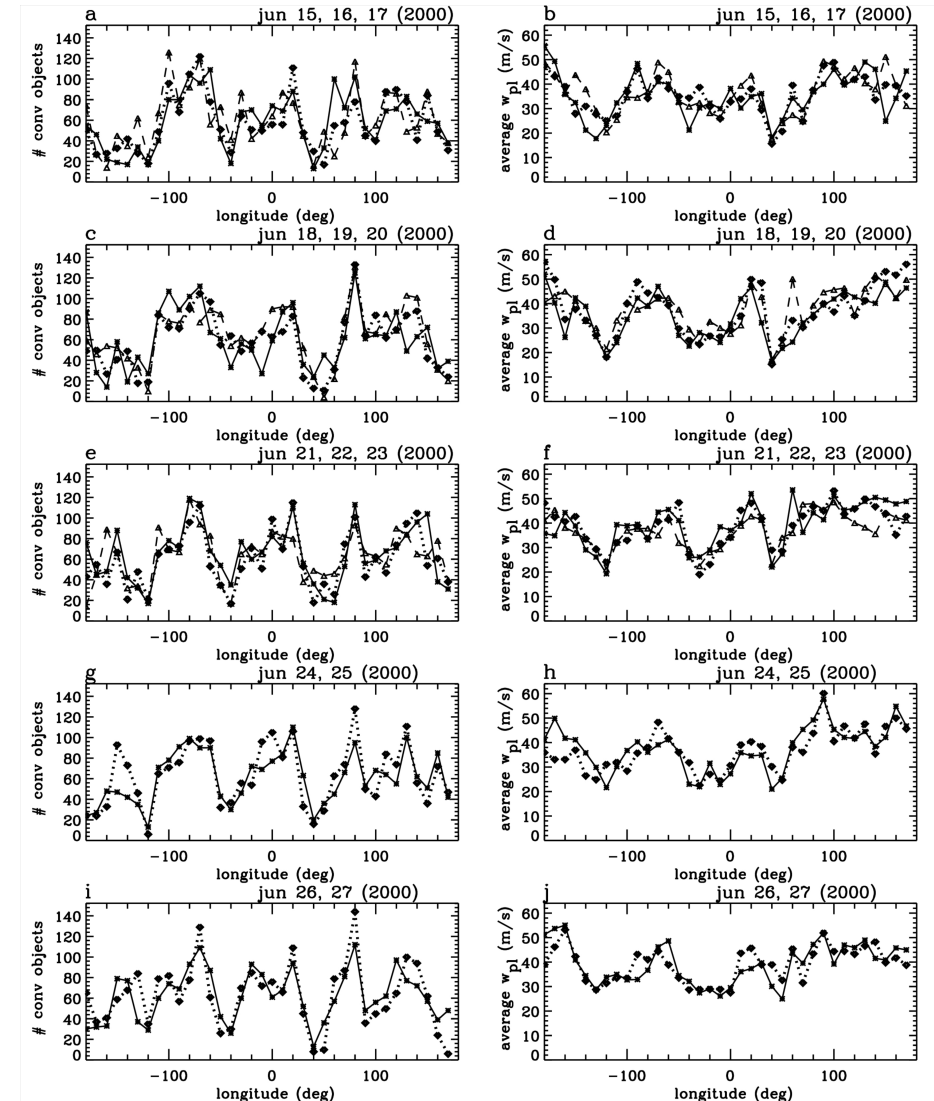
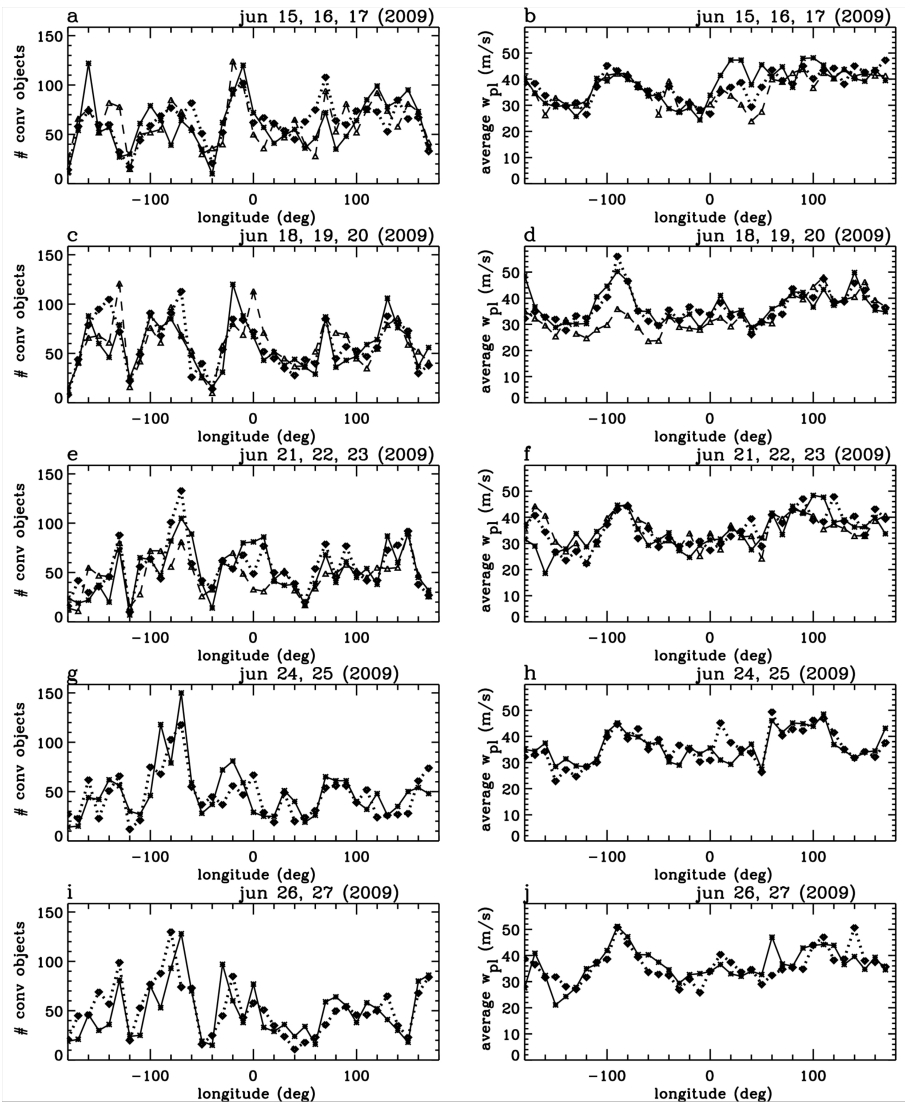
- The dissipation of GWs from deep convection induces horizontal wind perturbations at $z \sim 150\text{-}250$ km of $\sim 50\text{-}150$ m/s. These wind perturbations are significant up to $z \sim 400\text{-}500$ km. T' \sim few to 20 K.
- The changes from the heat/coolings associated with GW dissipation are mainly in the induced temperature perturbations. These perturbations are ~ 3 times smaller than T' from the thermospheric body forces
- GW dissipation in the thermosphere generates in-situ planetary scale waves in the thermosphere. (Mechanism: GW momentum fluxes are imprinted via wind filtering in mesosphere and lower thermosphere.)

Convective objects and updraft velocities are quite similar for extreme solar minimum and solar maximum.

This is not surprising, since the energy in the troposphere is much larger than the input energy from sun:

2009

2000

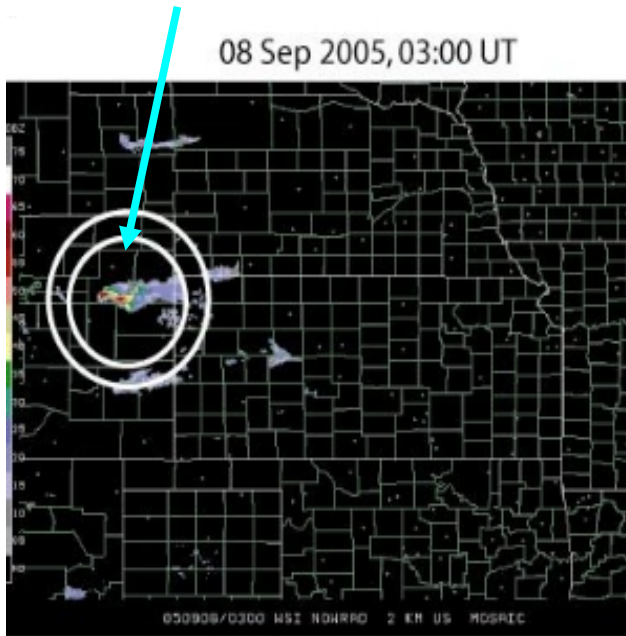
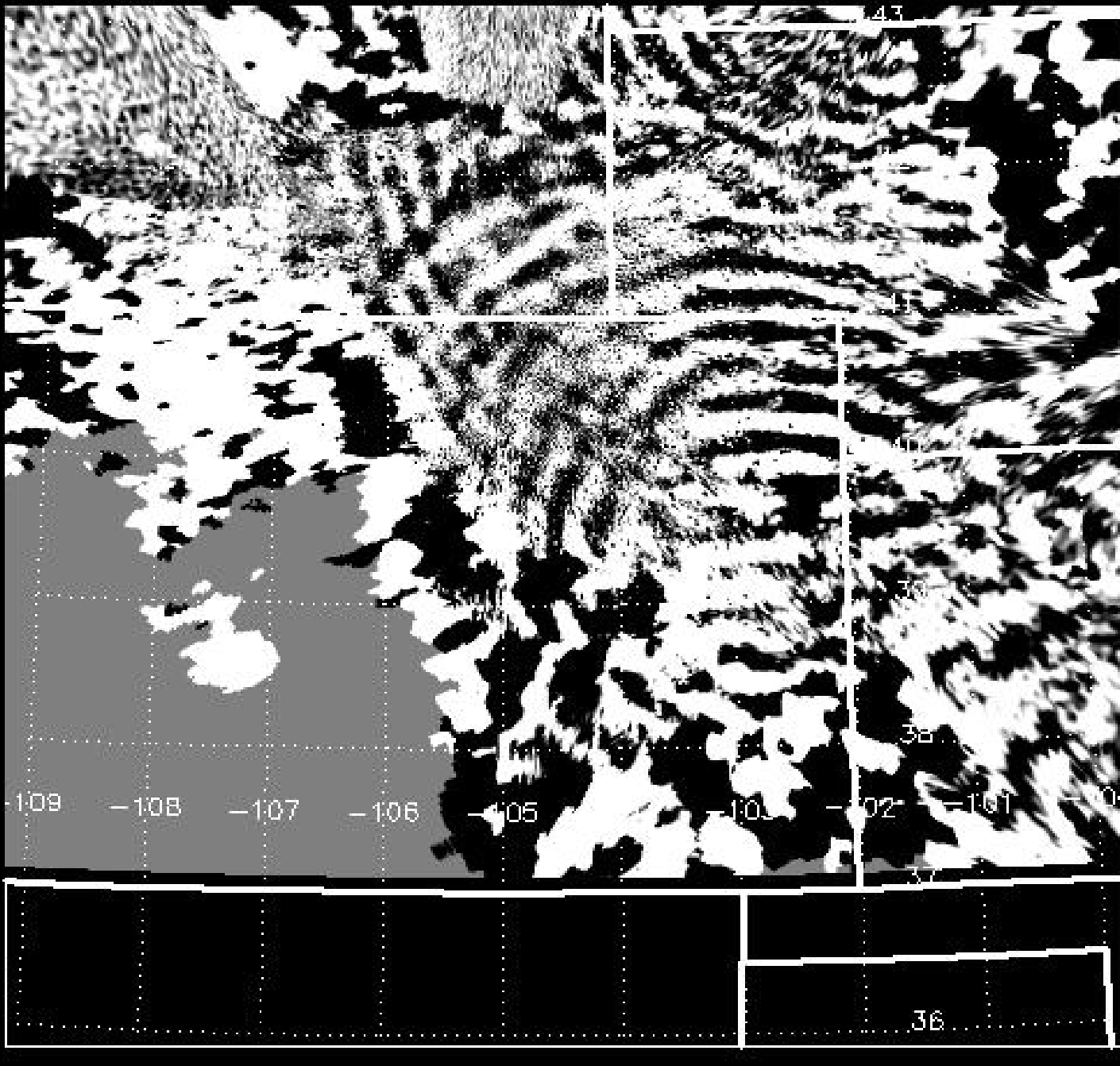


(Vadas, Liu, and Lieberman, 2014, JGR)

Yucca Ridge OH imager. Colorado 8 Sept, 2005

Observations of concentric Gws: Taylor and Hapgood, 1988; Dewan et al, 1998; Sentman et al, 2003; Suzuki et al, 2006; Yue et al, 2009

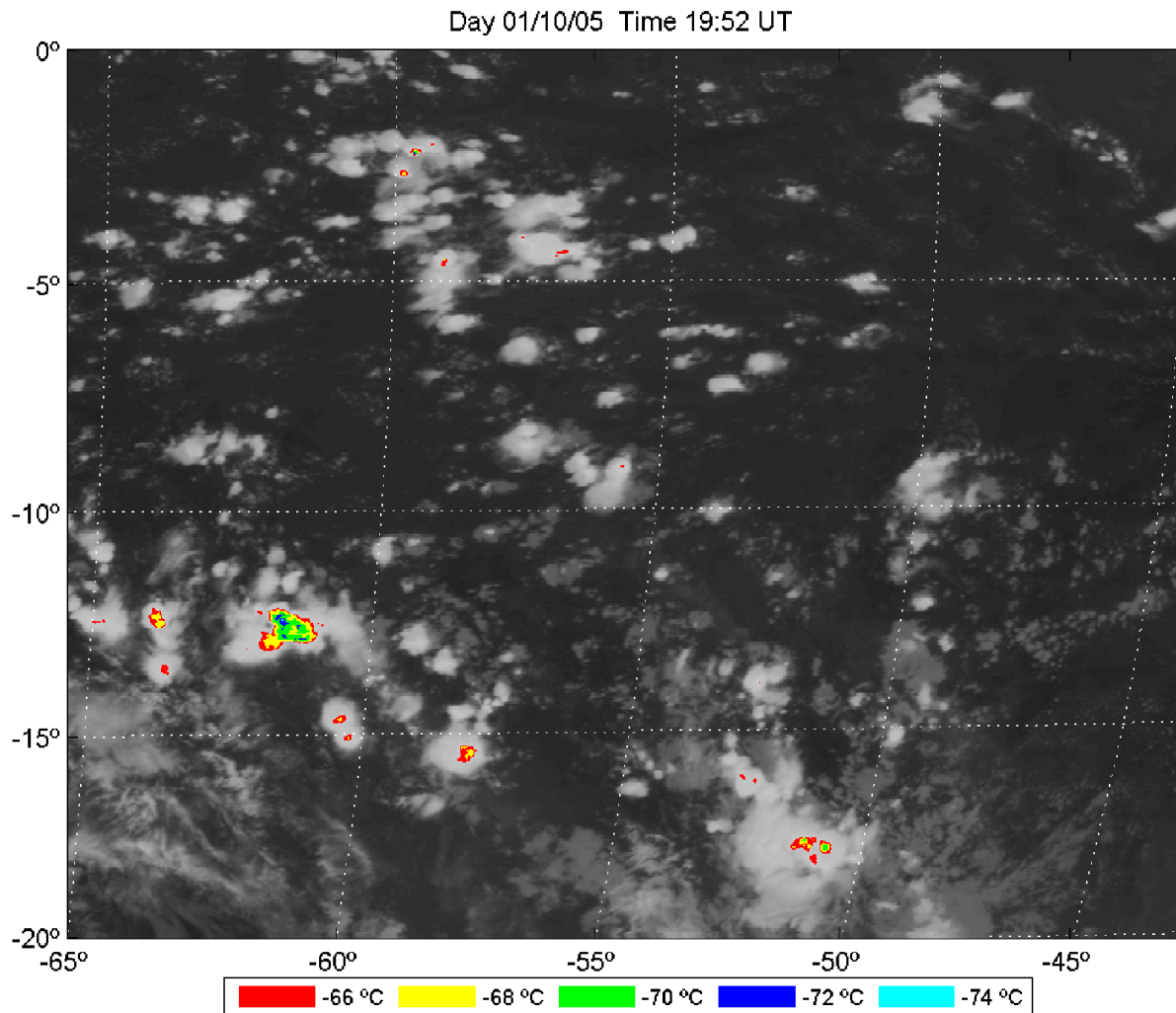
Overshooting convective plumes create concentric rings of gravity waves



(Coutesy of Jia Yue, Colorado State)

Yue et al (2009)

Model the local and global changes to thermosphere and ionosphere from 6 hrs of deep convection the evening of 01 October 2005



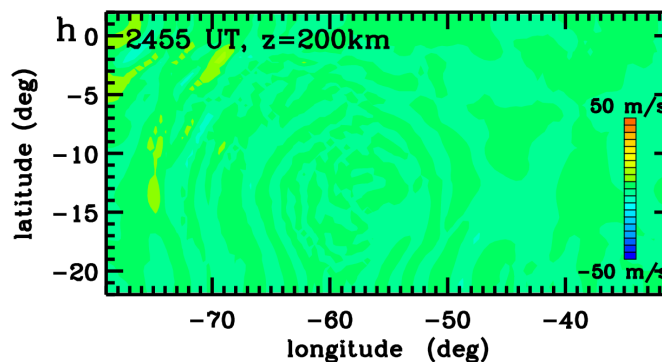
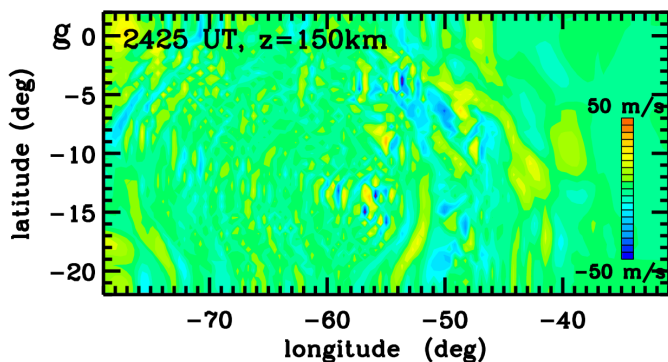
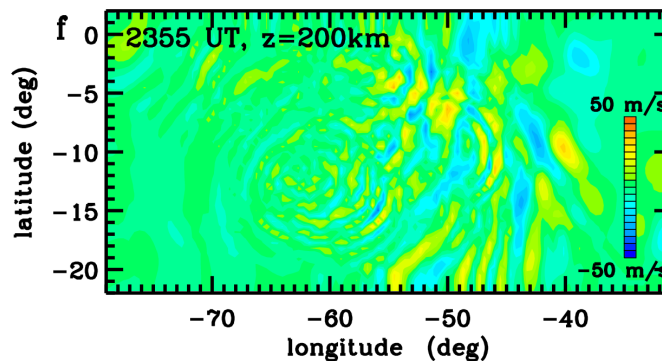
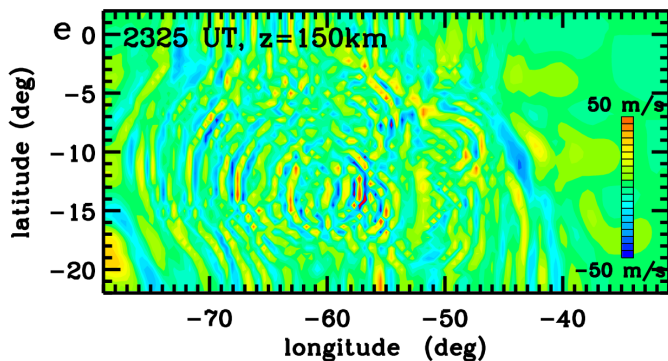
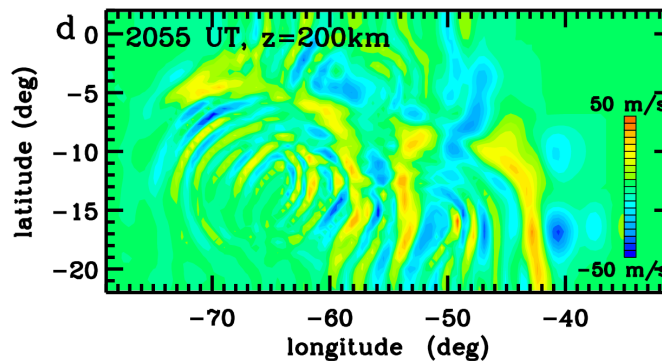
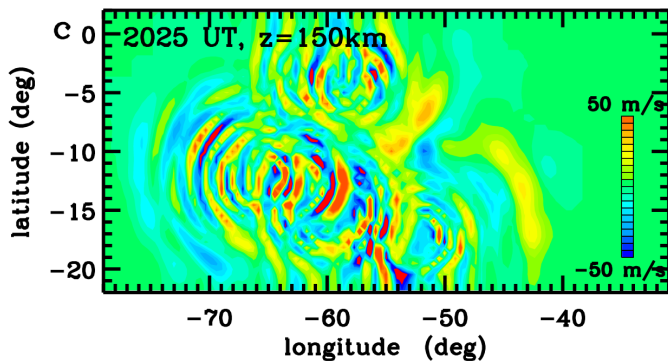
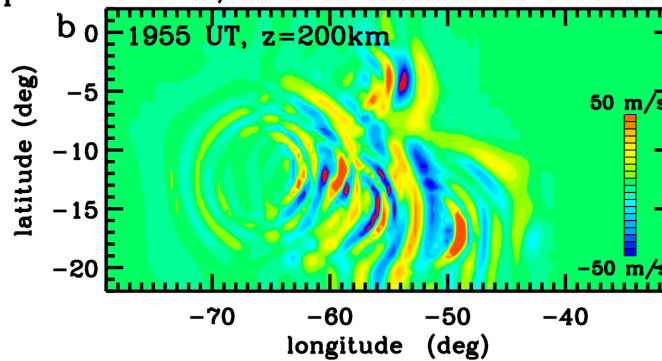
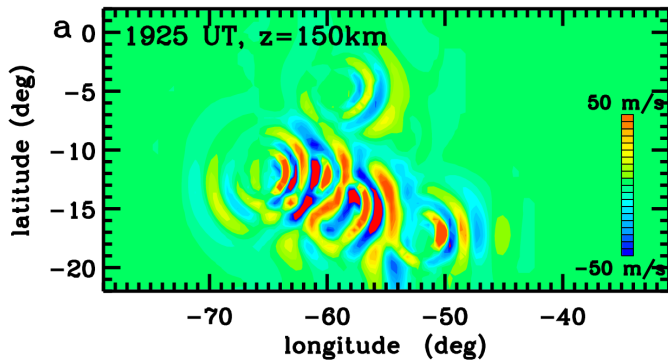
Model the GWs from several hundred plumes, clusters, and complexes

Goes-12 infrared satellite image at 19:52 UT over Brazil.

(Vadas and Liu, 2013, JGR)

Approach: determine the convective plumes which overshoot the tropopause, calculate the excited primary GW spectrum from each object, ray trace the GWs into the thermosphere where they dissipate, calculate the thermospheric body forces, and input these forces into the high-resolution TIME-GCM

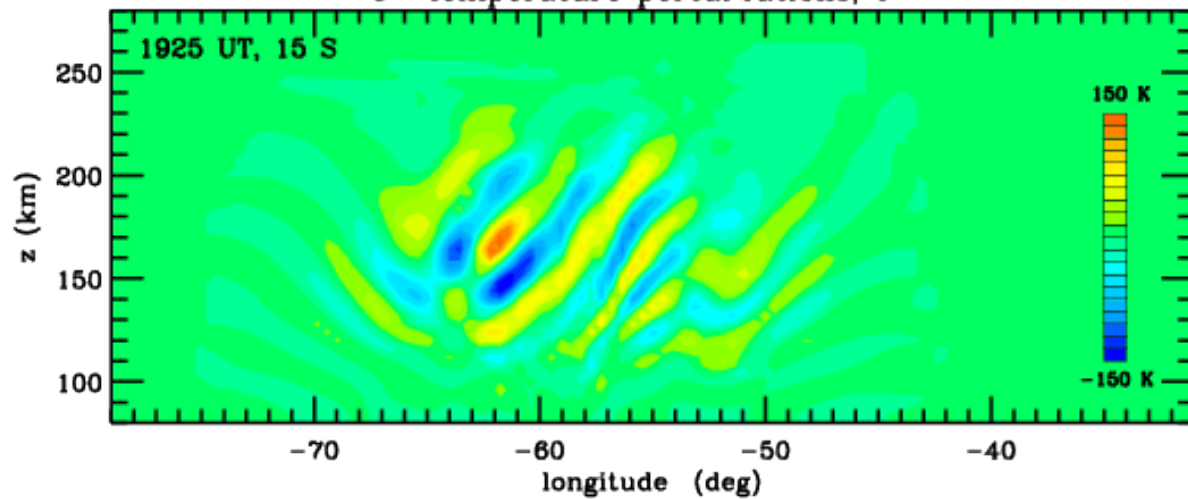
GW zonal velocity perturbations, u'



Reconstructed
primary GW zonal
velocity
perturbations
after ray tracing

Horizontal
wavelengths of
 $\lambda_H \sim 100-300$ km

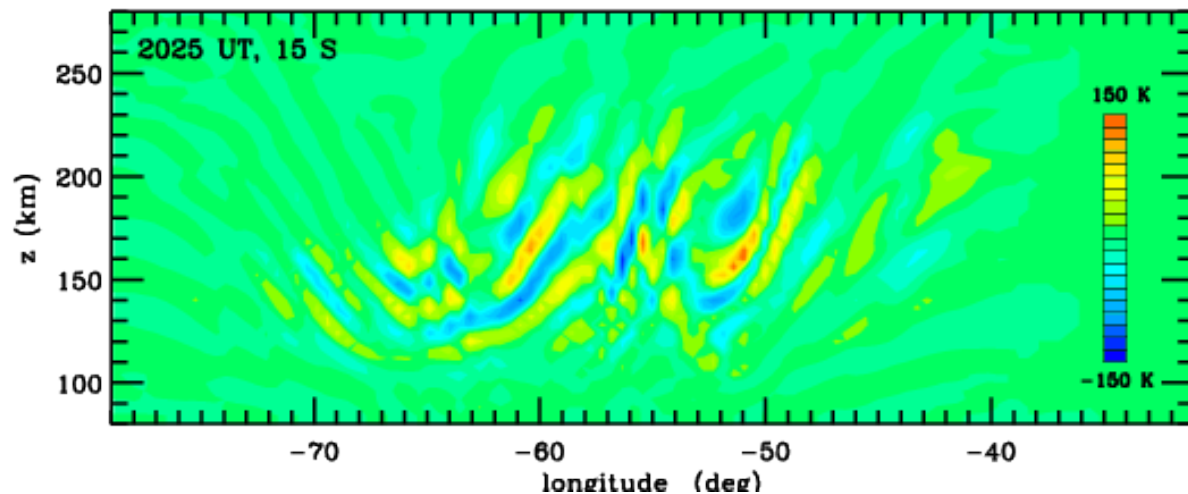
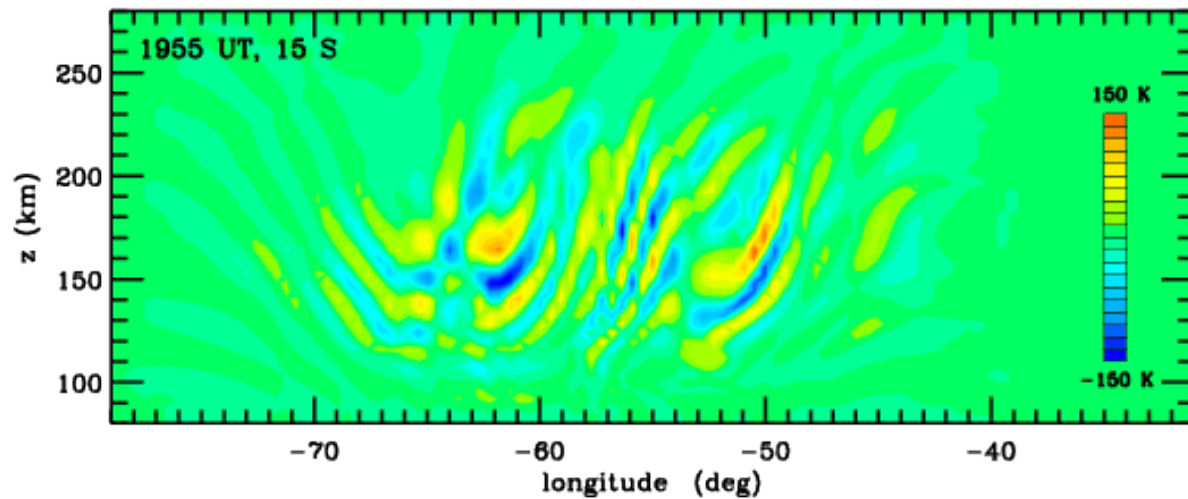
GW temperature perturbations, T'



Reconstructed temperature perturbations of the primary GWs at 15 S.

Note: amplitudes are small for $z > 220$ km.

λ_z is larger early, and is smaller later

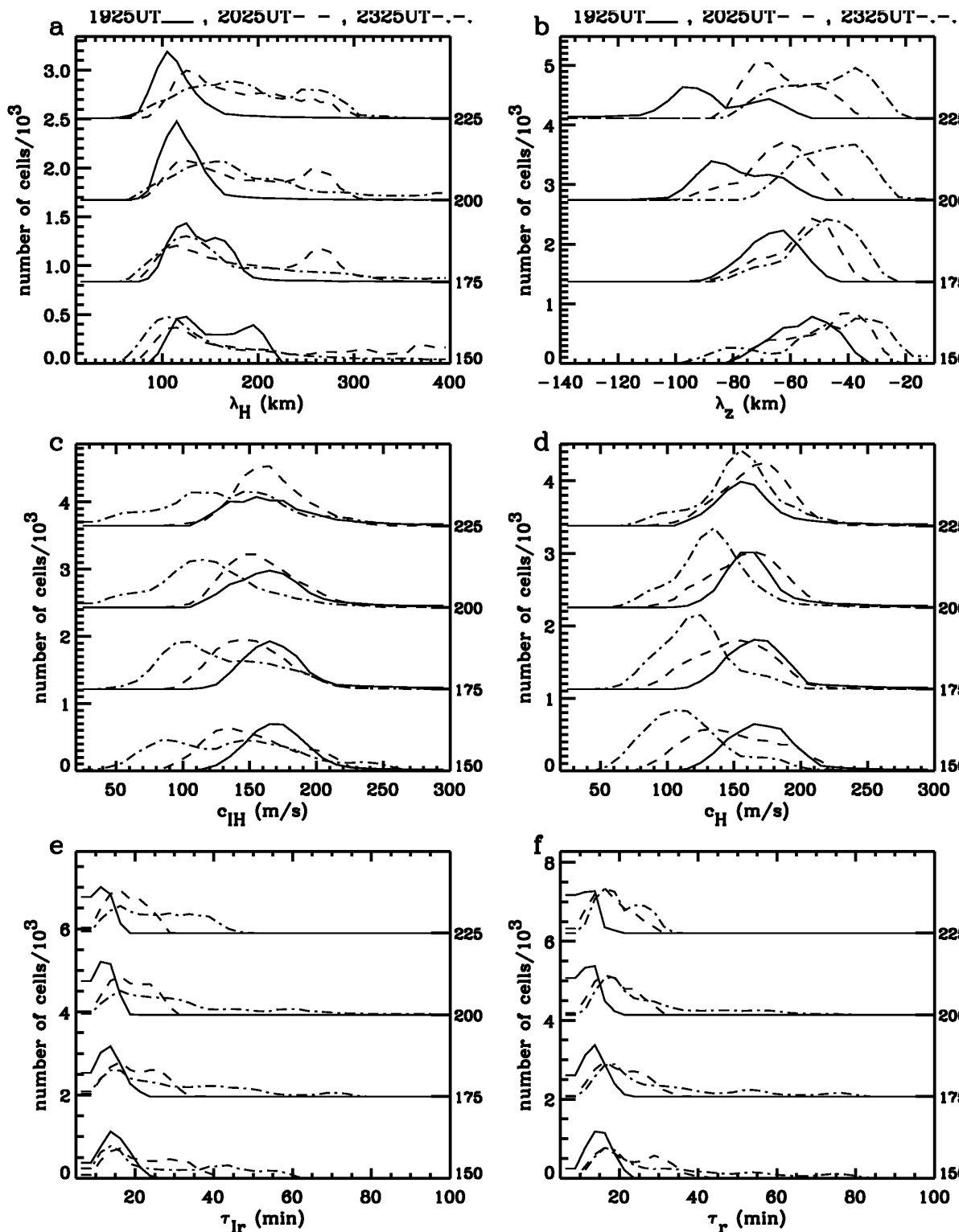


Characteristics of the primary GWs

Shown at $z=150, 175, 200$ and 225 km

19:25 UT (solid)
20:25 UT (dashed)
23:25 UT (dashed-dotted)

Horizontal wavelengths of
 $\lambda_H \sim 100-300$ km,
 $c_{IH} \sim 50-250$ m/s,
 $T_{ir} \sim 10-60$ min



(Vadas and Liu, 2013, JGR)